United Nations Environment Programme

Distr.
LIMITED

UNEP/CCOL/8/3/Add. 6
24 February 1986

Original: ENGLISH

Co-ordinating Committee
on the Ozone Layer

Eighth Session

Nairobi, 24-28 February 1986

RECENT RESEARCH RESULTS AND ONGOING AND PLANNED RESEARCH PROGRAMMES

Submitted by

Federal Republic of Germany

Planned and ongoing research activities:

In the Federal Republic of Germany, present research activities place special emphasis on field measurements of trace constituents of the atmosphere, on intercomparison of different measurement techniques with the aim to increase measurement accuracy, and on model development and comparison.

The Federal Republic of Germany contributed to the NASA/WMO assessment on atmospheric ozone and took part in several NASA workshops, including the ones on 'Model Assessment' and 'Model Predictions'.

For the future, the Federal Republic decided to continue the support for research on physico-chemical processes in the atmosphere; a subprogramme deals with research on the ozone layer.

Research proposals include the extension of balloon borne measurements to sulphur components, and light hydrocarbons for indirect assessment of OH and Cl concentrations, construction of high resolution interferometric apparatus, and extension of vertical ozone profile measurements to 50 km by differential absorption lidar techniques.

Ozone observations

A summary of the long term ozone profile measurements carried out by the Meteorological Observatory Hohenpeißenberg is displayed in fig. 1. The ozone decrease in the region of the maximum (22 km) continued in 1985, and so did the decrease in the region above 28 km that was first seen in 1977.

The sharply peaked decreases in the middle stratosphere that show up also as an absolute minimum in the total ozone record are suspected to be related to both the El Chichon volcanic eruption in April 1982 and the pacific 1982-83 El Nino. This depletion episode seemed to have terminated, however, in 1984. Since then, a renewed decrease was observed between 16 and 22 km.

The observatory will in future carry out routine ozone measurements up to 50 km for which a lidar system is now being installed. Work is carried out in close collaboration with the Physics section of the University of Munich that has, in the past two years, gained considerable experience with the differential absorption technique using a pulsed XeCl excimer laser operating at repetition rates of up to 100 Hz.
The laser radiation at 308 nm is strongly absorbed by ozone; as reference, light at 353 nm that is not absorbed by ozone is generated by stimulated Raman scattering. Below 30 km, ozone profiles with an accuracy of approximately 1 % are obtained in an averaging time of less than one hour. Above 40 km, averaging times of several hours are required for the same precision.
Fig. 2 and 3 show examples of the results obtained on the summit of the Zugspitze in the German Alps.

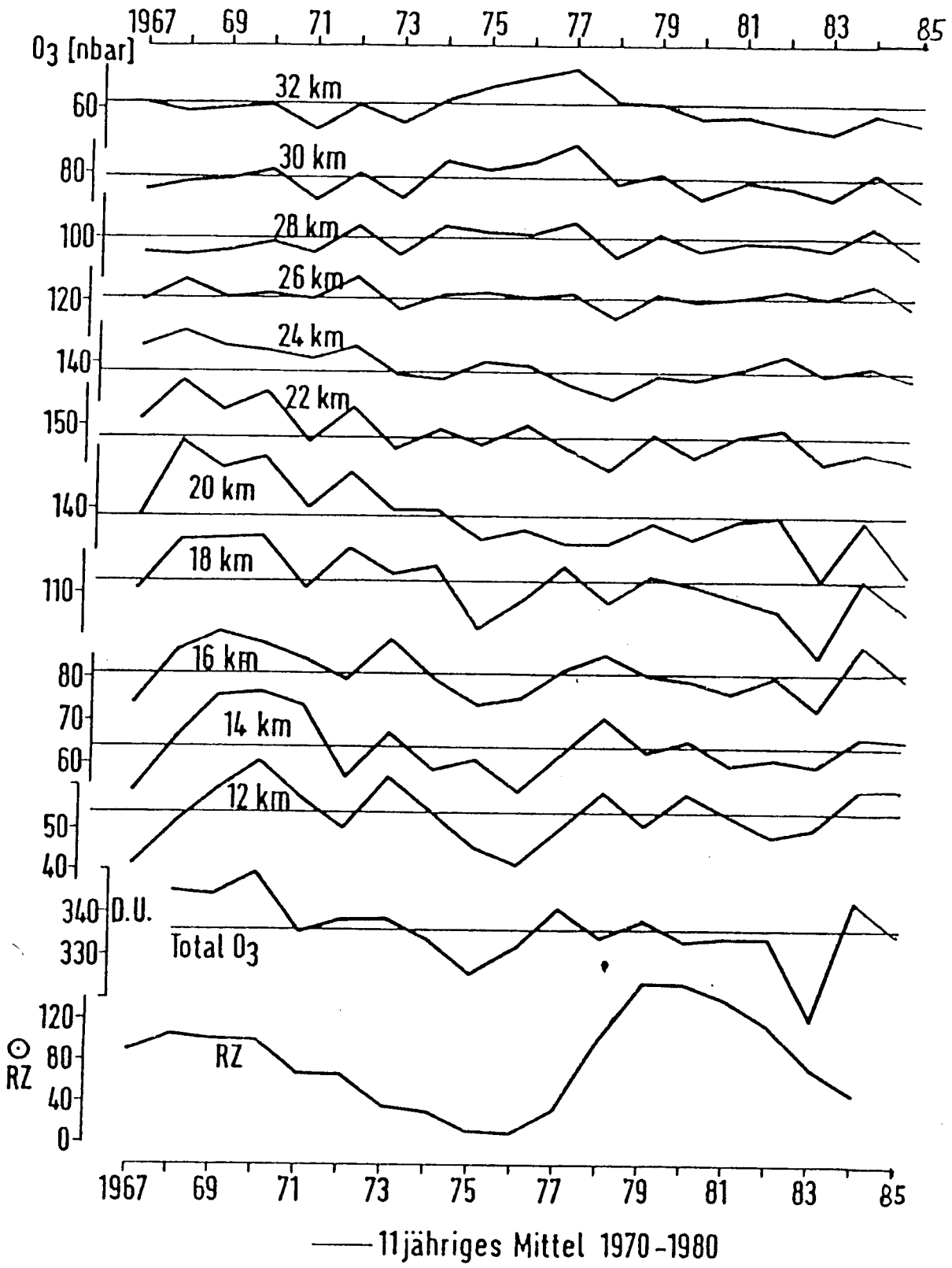

Fig. 1 : Yearly mean ozone profiles in the 12-32 km range together with total ozone and relative sunspot numbers, from 1967 to 1984.
(- 11 year mean 1970 to 1980)

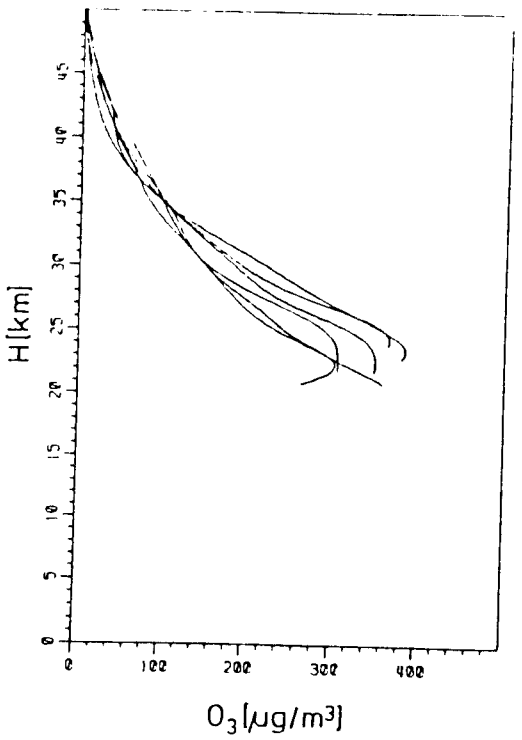

Fig. 2. Ozone density profiles measured in February 1983. Each profile represents the mean ozone concentration measured in one night

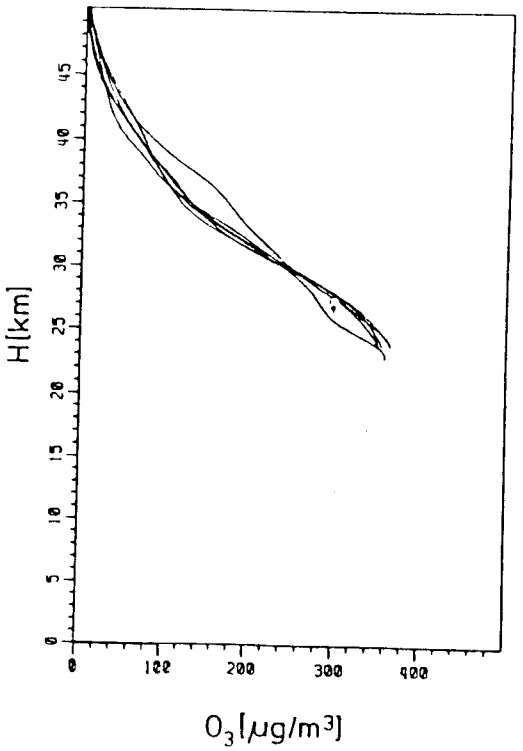

Fig. 3. Ozone density profiles measured in June 1983. Each profile represents the mean ozone concentration measured in one night

Vertical profiles of trace gases

The MPI for Aeronomy in Lindau and the KFA Jûlich have continued their measurements of vertical profiles of long lived trace gases. Large air samples are collected by balloon borne cryogenic samplers and subsequently analyzed by gaschromatographic methods in the lab. Results for CH_4,N_2O, and CFCl2 from a series of observations at 44°N during different times of the year are shown in figs. 4 a-c. The mixing ratios are lower in early winter (October 1982, 1985) than during the summer months. For one profile in March 1985, measured 10 days after the final stratospheric warming, a pronounced structure showed up with mixing ratios that were lower by factors of 1.3 to 3.0, depending on the species.

As part of the MAP-GLOBUS campaign, an intercomparison flight with samplers from both institutions was carried out in 1983. For CH_4,N_2O, and CFCl2, differences in concentrations were 5% to 7%, they were significantly larger for CFC 11. A vertical profile with CFC 113 measurements of both institutes is compared to 1-D model calculations in fig 4d.

Results have now been published on KFA Jülich's direct measurement method of free radicals: A balloon borne cryosampler collects free radicals and trace constituents that are trapped in a polycrystalline H_2O or D_2O matrix. The samples are stored below 83 K until the analysis in the laboratory by X-band ESR spectroscopy at 4 K.

NO_2 and HO_2 mixing ratios at 44°N are shown, together with previous measurements, in figs. 5 and 6.
It is important to note that this measurement technique seems at present to be the only in situ method capable of producing HO_2 concentration values in the lower stratosphere. The measurements of HO_2 concentrations are difficult to explain with the present accepted theory. They are higher than modelled concentrations by a factor of 2 at 35km, and by a factor of 10 at 25km, with the factor even increasing towards lower altitudes.
The Meteorological Institute of the University of Munich has successfully constructed an operational version of a Michelson interferometer for high resolution atmospheric trace gas measurements. At present, an improved version of the interferometer is tested which might, in future, be used in balloon experiments and space shuttle missions.

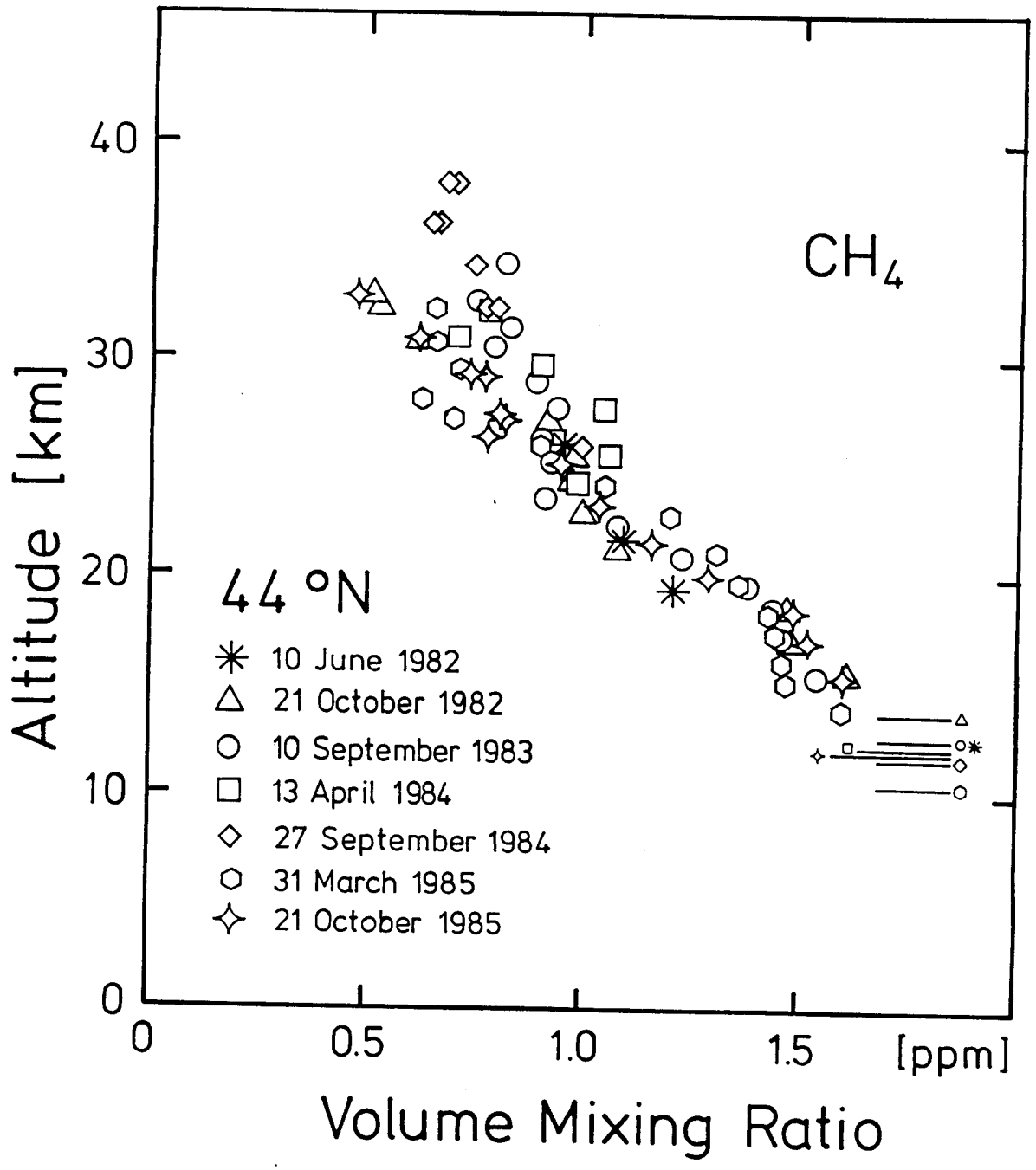
CH4
44 °N
10 June 1982
21 October 1982
10 September 1983
13 April 1984
27 September 1984
31 March 1985
21 October 1985
Altitude [km]
0
10
20
30
40
0
0.5
1.0
1.5
[ppm]
Volume Mixing Ratio

Fig 4a

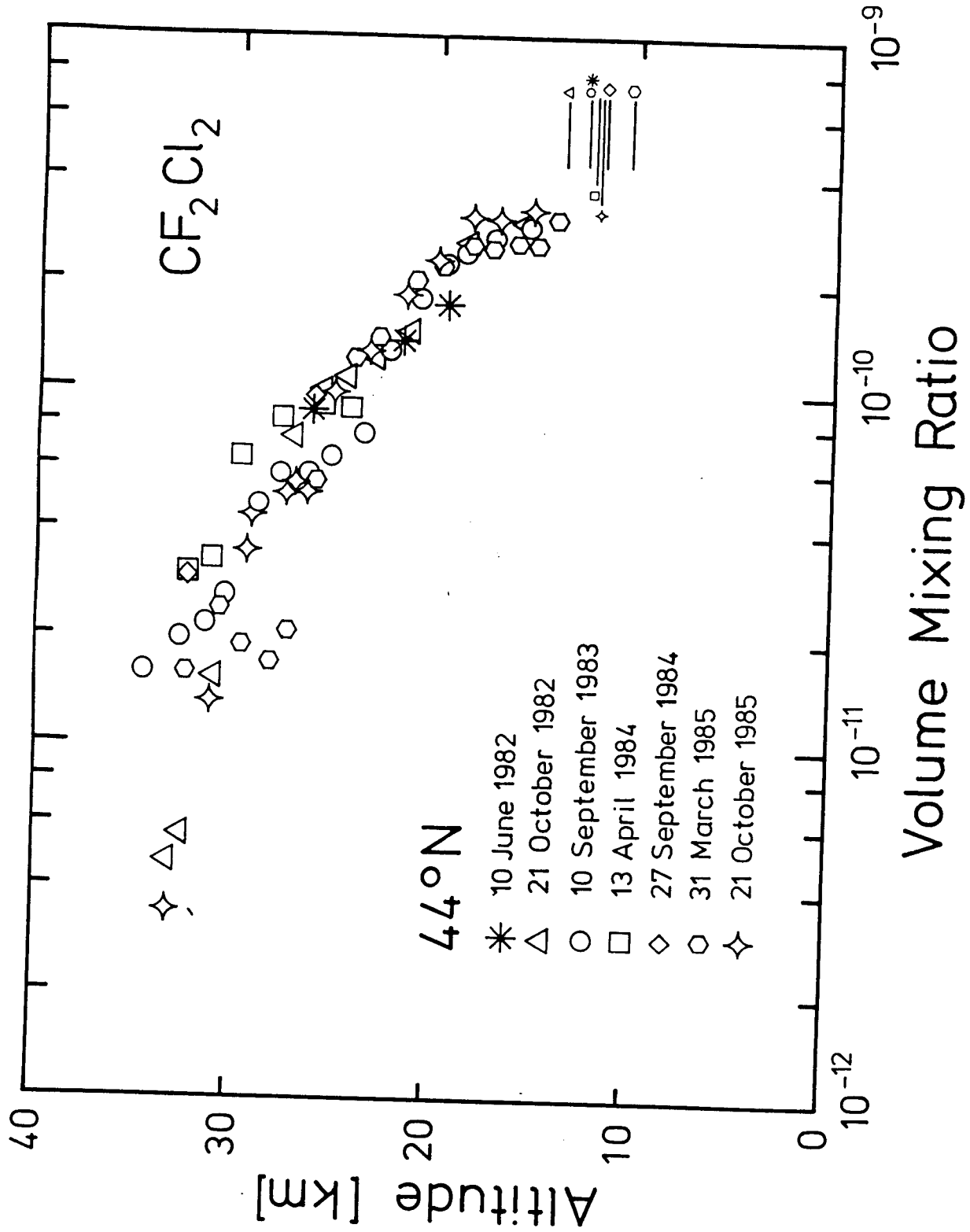
CF_2Cl_2
44°N
10 June 1982
21 October 1982
10 September 1983
13 April 1984
27 September 1984
31 March 1985
21 October 1985
Altitude [km]
Volume Mixing Ratio
0
10
20
30
40
10^{-12}
10^{-11}
10^{-10}
10^{-9}

Fig 4b

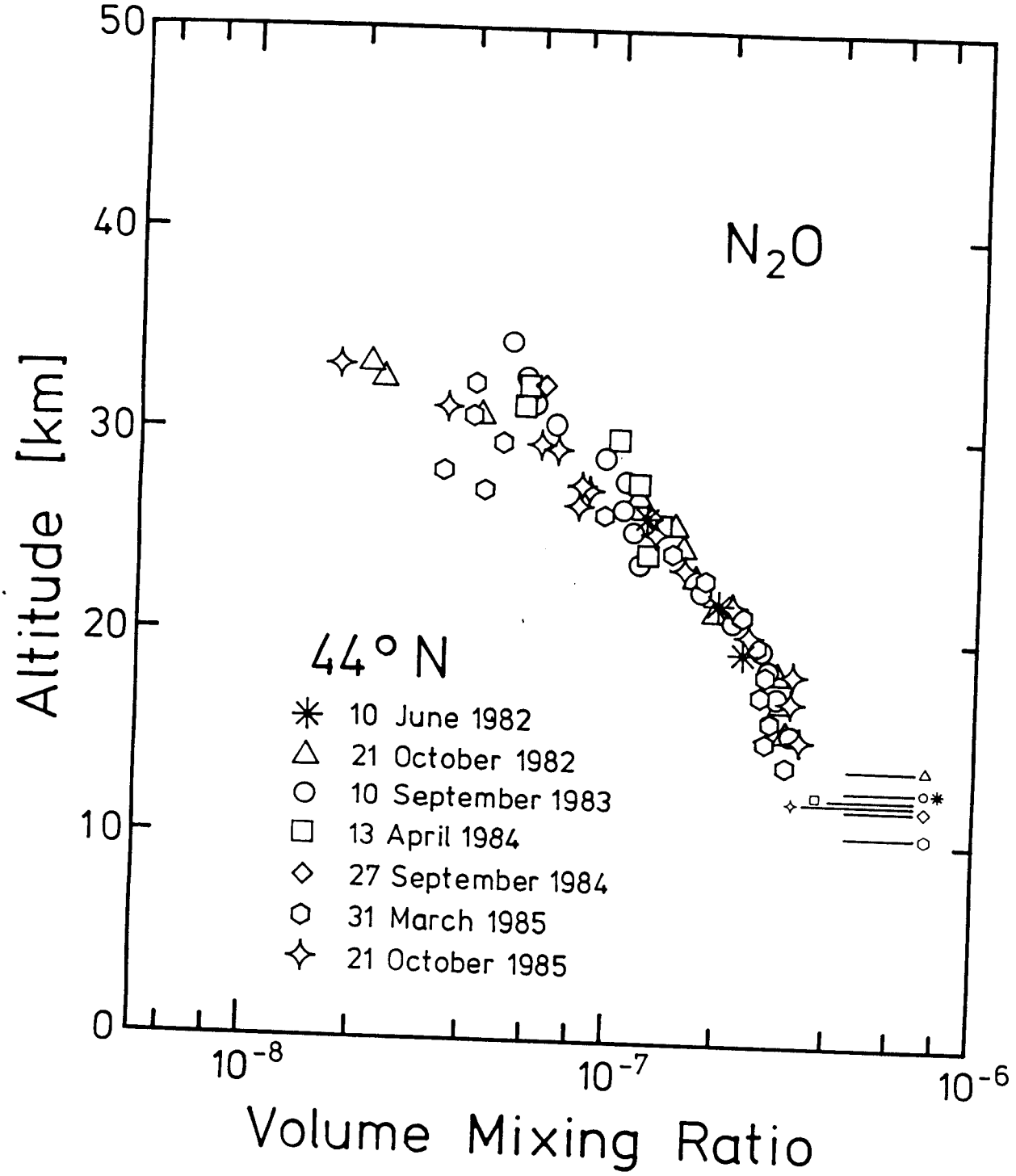
50
40
30
20
10
0
Altitude [km]
N_2O
44° N
10 June 1982
21 October 1982
10 September 1983
13 April 1984
27 September 1984
31 March 1985
21 October 1985
10^{-8}
10^{-7}
10^{-6}
Volume Mixing Ratio

Fig 4c

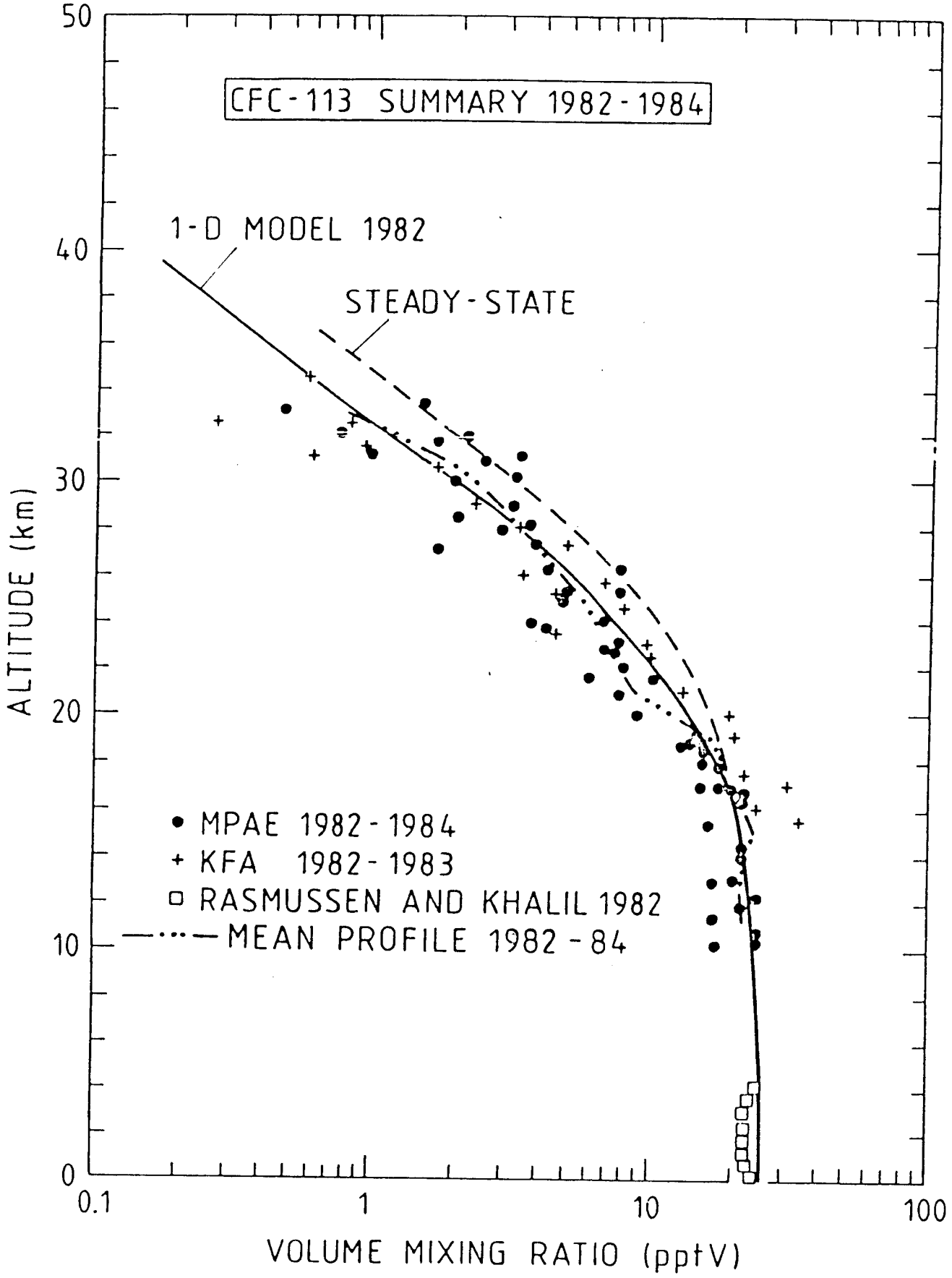

Fig. 4 a CFC-113 vertical distribution: summary 1982-84. The average profile was obtained by averaging all data points over 2-km height intervals.

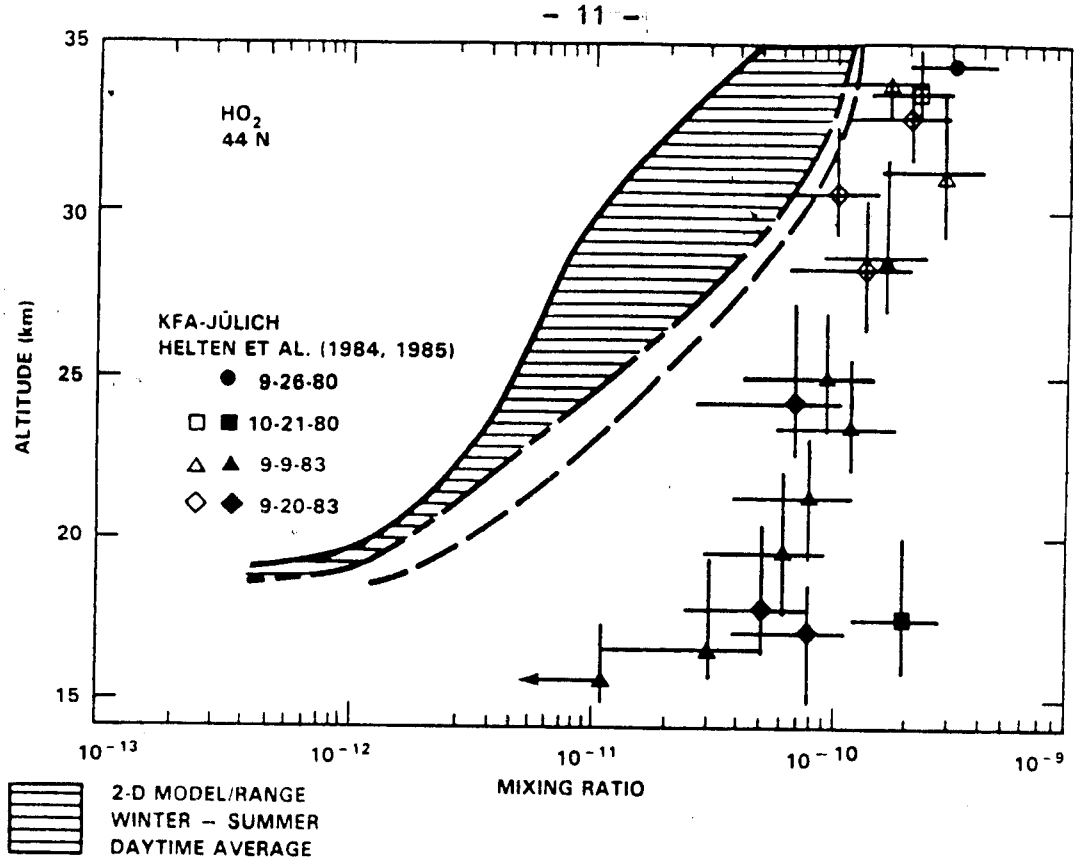

Figure 5. In situ observations of HO_2, employing the matrix isolation technique of Helten *et al.* (1984). The samples were collected during several balloon flights at local time between sunrise and approximately noontime. Data for observations made within 3 hours after sunrise are plotted with open symbols, because they should be adjusted due to the rather strong diurnal variation of HO_2 within this time period. The zenith angle for these samples are as follows: a: 88.1-78.1; b: 62.3-53.3; c: 95.8-83.9; d: 55.0-46.6; e: 86.8-77.2; f: 80.7-70.5. The dashed line represents a typical altitude profile for HO_2 calculated by Prather ( ).

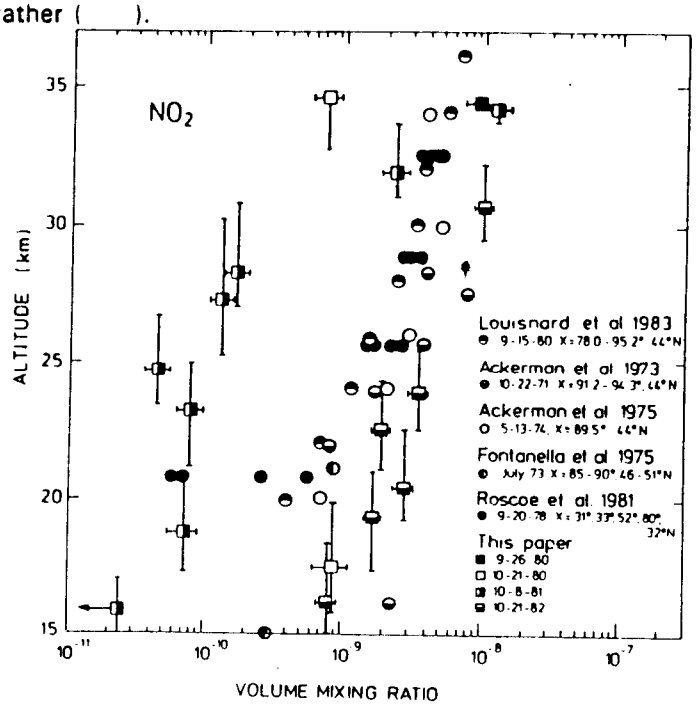

Fig. 6 Comparison of the present measurements of stratospheric NO_2 with earlier data. The vertical bars indicate the vertical sampling interval. The horizontal bars give the measurement error (for our measurements only). The symbols mark the altitude where the median amount was sampled.

Temperature in the middle stratosphere

Results of model calculations indicate a stratospheric temperature decrease as a consequence of increasing CO_2. The Free University of Berlin has continued its analysis of temperature data; taking daily radiosonde observations from 1966 to 1980, a negative trend of -0,24 K/decade is obtained as an area weighted average in the latitude band from $10^{o}N$ to $90^{o}N$ at the 30 mb level.
Since 1980, a rapid temperature increase has been observed, probably related to volcanic eruption, (Mt.St. Helens, El Chichon), with a hint of a renewed cooling in 1984 (fig. 7).

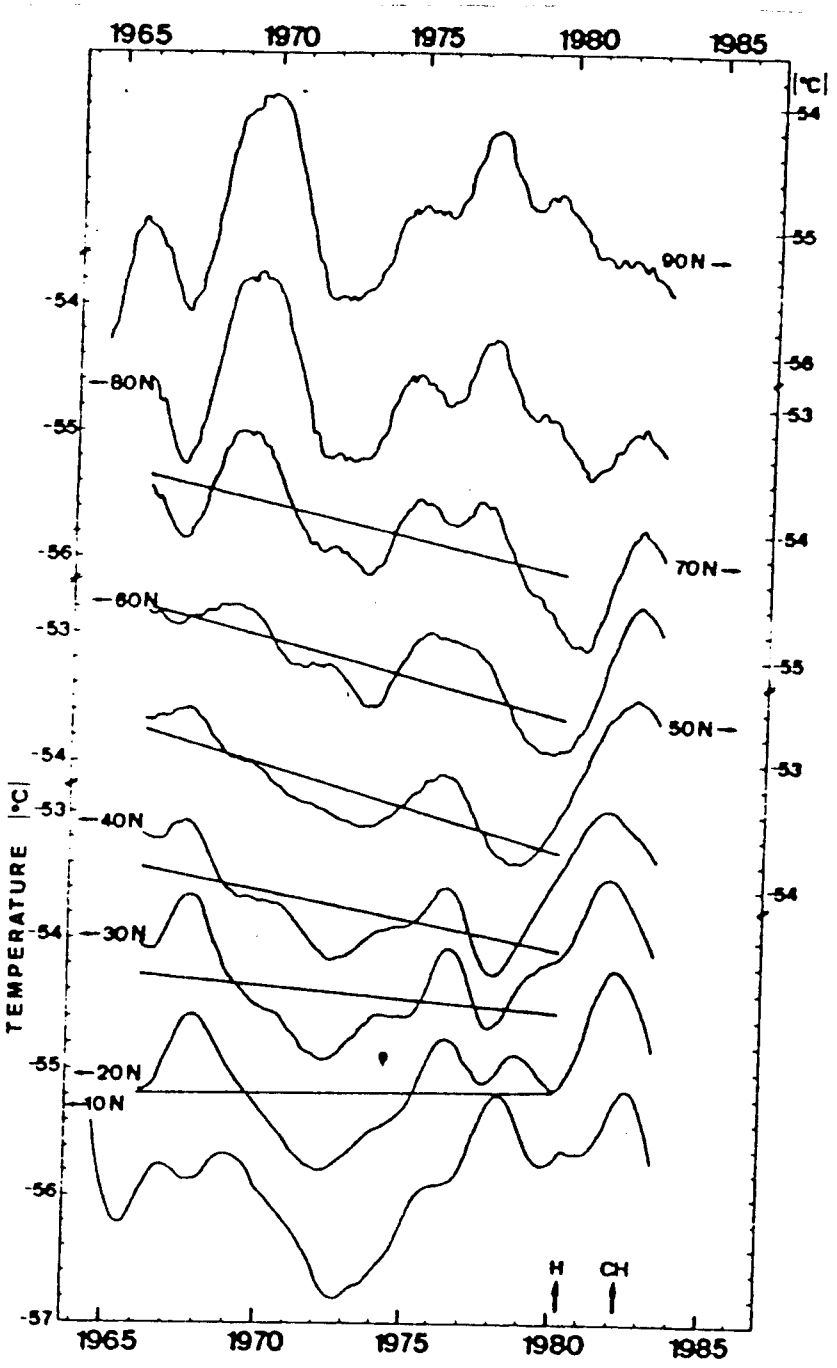

Fig. 7 : Middle stratospheric temperature trends, 1966-1984

Modelling results

The Max Planck Institute for the Chemistry of the Atmosphere in Mainz has carried out a number of model calculations:

a) Global profiles of halogenated hydrocarbons:

In cooperation with the Max Planck Institute in Lindau and the Rutherford Appleton Laboratory, Oxford, one-dimensional and two-dimensional profiles of CH_3Cl, CH_3Br, CCl_4, CFC14, CFC16, CFC12, CFC11, CFC22, CH_3CCl_3, CFC113, CFC114, CFC115, CFC13, CF_3Br, CF_2ClBr were calculated using specially compiled emission scenarios that start in 1920.

Profiles and ground values were compared to all available measurements. Significant differences among model results and between model predictions and measurements arose only with shorter lived species (CH_3CCl_3, CFC22, CCl_4).

b) Budget of stratospheric ozone:

Ozone budget calculations using trace gas concentration measurements from the LIMS and SAMS satellite experiments suggested that a modified ozone production rate would eliminate the present budget discrepancy in the 30 - 40 km vertical range.

c) International comparison workshop:

The NASA workshop 'Model Assessment', for which calculations with the two dimensional Eulerian model were carried out, revealed significant differences of odd-nitrogen predictions between the different models. This is attributable, for predictions in the upper statosphere, to differences in NO photodissociation modelling, and in the lower atmosphere, to differences in transport in transport and troposheric chemistry modelling.

For the NASA workshop 'Modelling Predictions', the MPI's Eulerian model was one of three models chosen to predict ozone concentrations for different given steady state scenarios. All models predict the maximum ozone depletion in the vertical 40 - 45 km range, for all scenarios.

The larger depletions in total ozone occur for higher latitudes. For specific latitudes and seasons, the maximum change in the ozone column can differ by as much as 100% from the mean global change.

Generally, 2D models predict higher mean ozone depletions than 1D models that use tne same chemical reaction kinetics. For example, 2D models give a 9% ozone reduction with 1980 from emissions compared to 5% - 7% for 1D models. 2D models show an approximately linear relationships between chlorine concentrations and ozone depletion in contrast to 1D models which predict a more than proportional reduction.

d) Results from a coupled 1D climate-photochemistry model:

The possible impact on climate and the ozone layer of trace gas emissions can now be investigated with a coupled climate-photochemistry model, both for steady state scenarios and time dependent calculations. Results indicate that the CFC greenhouse effect increases the temperature in the cloudless troposphere and lower stratosphere by 0,7 K (fig. 9).

The resulting higher water vapour and O (1D) concentrations cause higher total ozone depletions via troposphere odd-hydrogen reactions even though the temperature effect reduces ozone depletion in the stratosphere. In the model, increasing CO_2 concentrations therefore have little effect on ozone:

The reduction in stratospheric ozone depletion by the lower temperatures is compensated by water vapour induced tropospheric ozone depletion. In contrast, CH_4 plays a major role: Doubling the CH_4 concentrations reduces the ozone depletion significantly.

Time dependent calculations with increasing CH_4, CO_2, N_2O and CIX, but constant CO and NO_x emissions yield an ozone increase of 1,5% from 1860 to 1960, a subsequent decrease of 2% by 2020, and again an increase thereafter; this presupposes constant CFC emissions from 1984 onwards.

Different results are obtained, however, when increasing CFC emissions are assumed: A yearly increase of 4% - in spite of also increasing CO and NO_x emissions - results in ozone reductions of around 20% by 2050 - increasing tropospheric ozone cannot, in this case, compensate the calculated 70% reduction in the 40 km range (fig. 8).

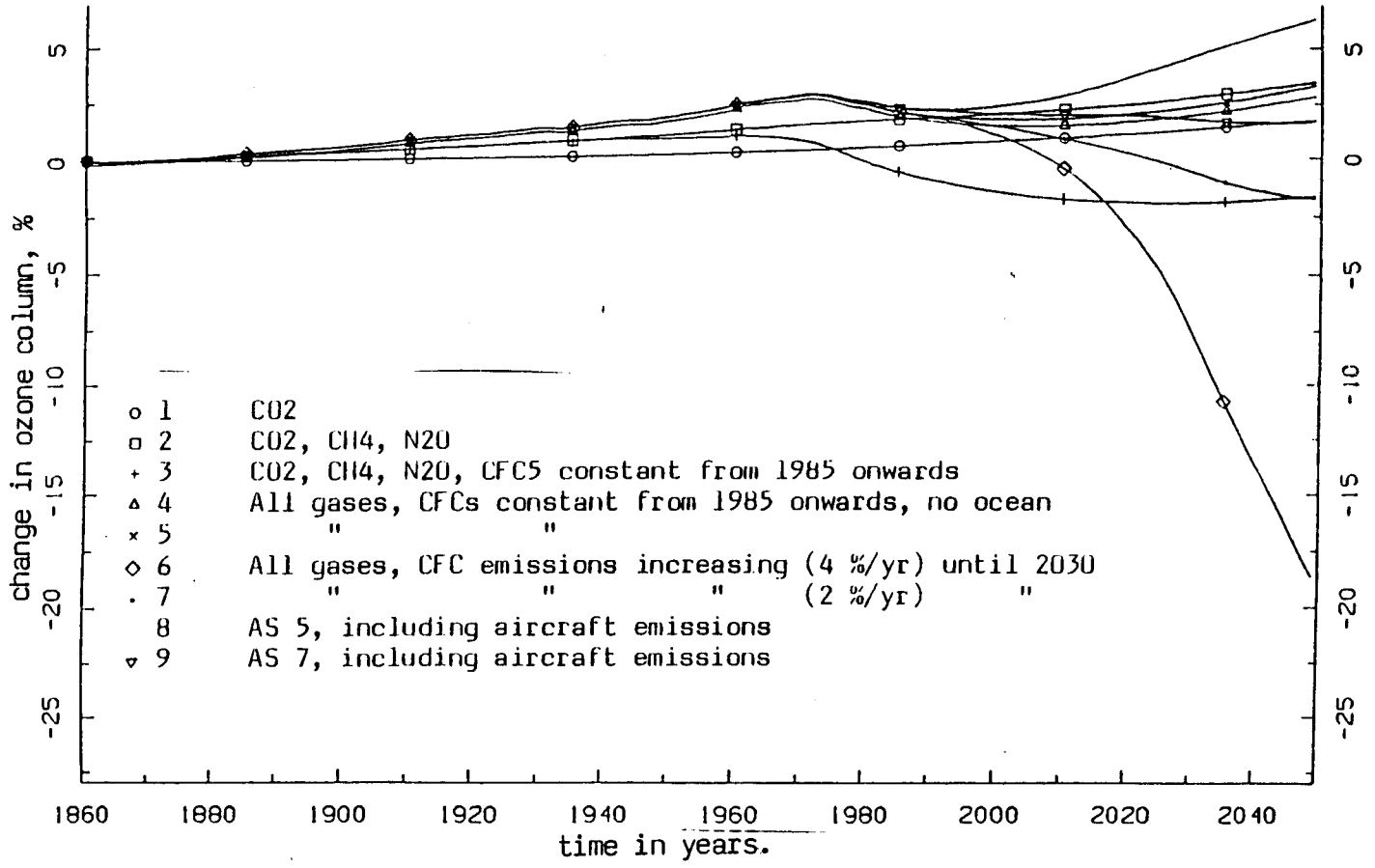

Fig. 8 : Change in ozone column for different scenarios

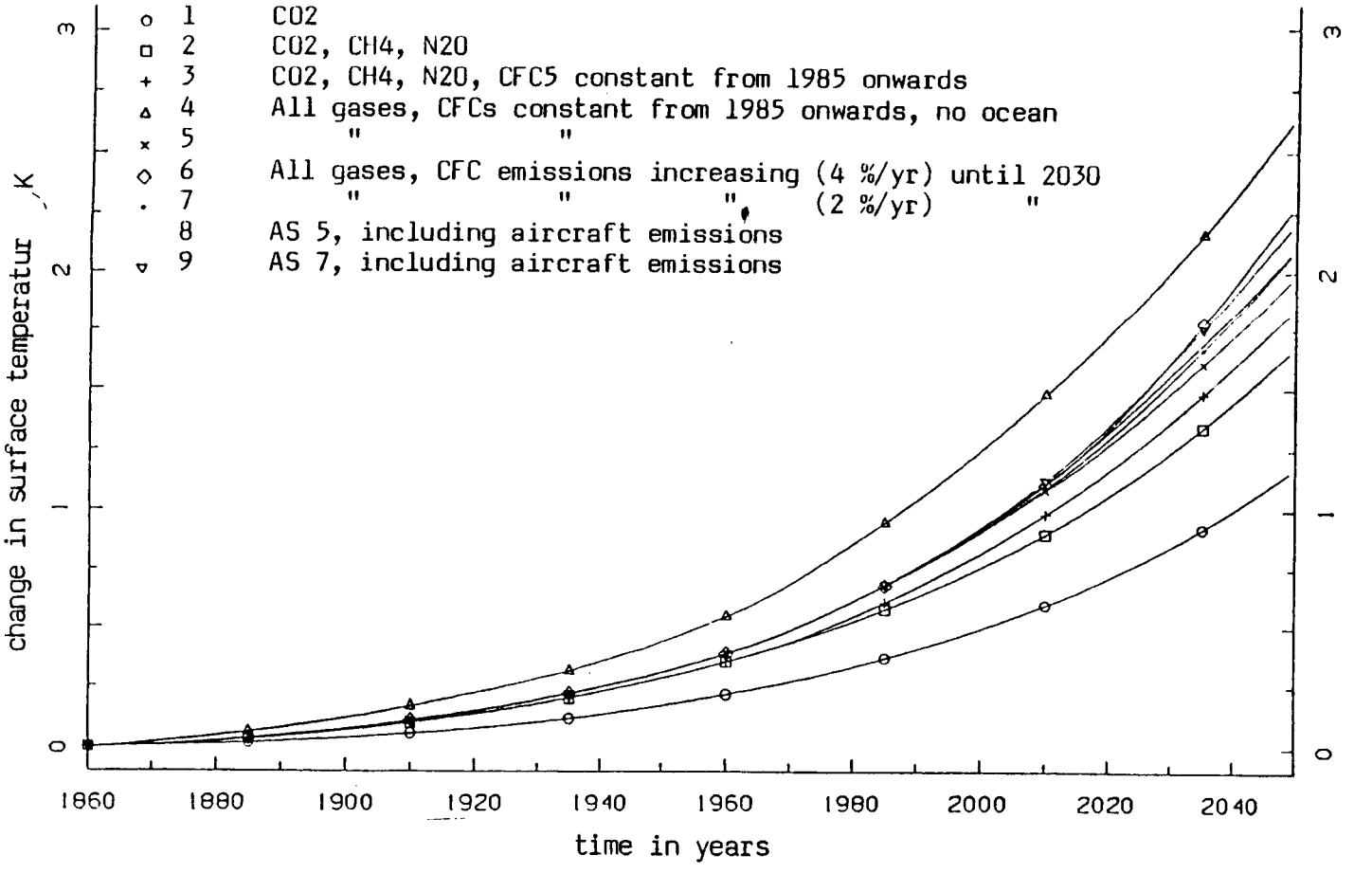

Fig. 9 : Change in surface temperature for different scenarios